Avrupa Bilim ve Teknoloji Dergisi
Sayı 14, S. 90-95, Aralık 2018

Araştırma Makalesi

www.ejosat.com ISSN:2148-2683

European Journal of Science and Technology
No. 14, pp. 90-95, December 2018

Research Article

Attenuation Parameters and Effective Atomic Numbers of Concretes Containing Pumice for Some Photon Energies by Experiment, Simulation and Calculation

Hakan Akyıldırım[1*]

[1] Süleyman Demirel University, Science and Arts Faculty, Physics Department, 32200, Isparta-Turkey

(First received 20 August 2018 and in final form 5 November 2018)

(DOI: 10.31590/ejosat.454777)

Abstract

Photon mass attenuation coefficients and effective atomic numbers for three types of concretes containing pumice mineral in different rates (namely 0%, 50% and 100%) were studied by photon transmission experiments, by simulations and by theoretical calculations. Experimental procedure was realized by using a 3″×3″ NaI(Tl) connected to a 16k multichannel analyzer detector system for 511, 835 and 1275 keV photon energies. In simulations, Geant4 Monte Carlo simulation toolkit was used to estimate the total mass attenuation coefficients via total linear attenuation coefficients. For theoretical calculations, web version of XCOM code was used at 1 keV – 100 GeV energy region for comparison. Also, mean free paths and half value layer thicknesses of concretes were calculated at this energies by means of attenuation coefficients obtained by three methods. Results from each method were found to be in a reasonably good agreement. Besides, it was concluded that addition of heavy weight elements to concrete effected attenuation parameters positively.

Keywords: Photon attenuation, effective atomic numbers, Geant4, XCOM, pumice concrete.

1. Introduction

Radiation protection became one of the most important subjects of recent decades because radioactive materials had various fields of usage from health to space study missions and so it is a significant task to protect living organisms and other systems against the harmful effects of ionizing radiations such as gamma-rays. So, it is necessary to apply proper shielding to avoid these harmful effects. Effectiveness of a shielding material against gamma-rays is measured by means of the total linear attenuation coefficient (μ) which is defined as the interaction probability of a photon per unit distance of the medium it traverses. In microscopic scale, μ is the sum of partial cross section contributions from three main interactions, which are photoelectric effect, Compton scattering (or incoherent scattering) and pair production in the field of nucleus as follows (Hubbell, 1982; Jaeger, 1965):

$$\mu = \mu_{pe} + \mu_{scatt} + \mu_{pp} = \frac{\rho N_A}{A}\sigma_a \quad (1)$$

Here, N_A is the Avogadro's number, ρ, A and σ_a are the density, atomic weight and total atomic cross section of the material of interest, respectively. Each type of interaction is dominant at different energy regions, so, the value of total linear attenuation is strongly related to photon energy. Besides this, atomic number and density of the material are the two other factors effecting the attenuation coefficient positively. Therefore, for appropriate shielding against gamma-rays of any energy, it is required to use materials with high atomic number and density.

In a well-designed experiment or a simulation, when a collimated beam of monochromatic photons with an intensity of I_o impinges on a material of thickness x, a portion of the beam photons interacts with the material via aforementioned photonic interactions which cause a decrease in the initial intensity. Calling the transmitted intensity as I, the total linear attenuation is given by the following formula (Price et al., 1957; Woods, 1982):

$$\mu = \frac{1}{x}\ln\frac{I_o}{I} \quad (2)$$

Besides the total linear attenuation coefficient, derived parameters from it, mass attenuation coefficient, mean free path (*mfp*) and half value layer (*HVL*) thicknesses are also other significant photon shielding parameters in radiation research literature. The total mass attenuation coefficient is simply the ratio of the total linear attenuation coefficient given by Equation 1 with respect to density of the material. So, it is independent of the density and physical state of the material of interest and this feature brings a significant advantage with it when theoretical calculation is in question. The total mass attenuation coefficients of compounds or mixtures such as alloys or concretes are calculated in accordance with the mixture rule. According to this rule, the total mass attenuation coefficient is the sum of individual contributions from the constituents as expressed in Equation 3, where w_i is the weight fraction and $(\mu/\rho)_i$ is the mass attenuation

[1] Corresponding Author: Süleyman Demirel University, Science and Arts Faculty, Physics Department, 32200, Isparta-Turkey, hakanakyildirim@sdu.edu.tr

coefficient of the i^{th} element in that compound/mixture (Hubbell, 1982; Berger et al., 2010).

$$\frac{\mu}{\rho} = \sum_i w_i \left(\frac{\mu}{\rho}\right)_i \quad (3)$$

Mean free path represents the average distance that a photon can travel between successive interactions and is calculated by

$$mfp = \frac{1}{\mu} \quad (4)$$

equation. Half value layer thickness is defined as the thickness of the material to reduce the intensity of incoming beam to half of the initial value and it is related to linear attenuation coefficient by following equation (Chilton et al., 1984):

$$HVL = \frac{\ln 2}{\mu} \quad (5)$$

The other fundamental radiation shielding parameter investigated in this paper is the effective atomic number (Z_{eff}) that is calculated in the case when the shielding material is either a compound or a mixture, such as concrete. Z_{eff} gives a convenient way to compare the attenuation characteristics of a compound/mixture with an element in the context of atomic number at a particular photon energy. So, the compound/mixture is considered as an element of atomic number of Z_{eff} for that particular energy. Theoretical background and notion of this parameter were first suggested by Hine (1952) who pointed out that since mixtures and compounds are composed of several elements, related Z_{eff} may not be represented by a single number. This means that in such materials photon attenuation cannot be expressed by a unique atomic number across the entire energy range, as it is in the case of pure elements. Keeping this point in view, it can be concluded that the effective atomic number of a compound/mixture is not constant, but should vary with photon energy. Evaluation of Z_{eff} of a compound/mixture at a particular energy requires the knowledge of the photon interaction cross section and finding out the pure element that has the equivalent cross section (Kumar and Reddy, 1997; Murty et al., 2000; Un and Demir, 2013; Elmahrough et l., 2015; Akman et al., 2015).

In this paper, results of a study on determination of aforementioned radiation shielding parameters for some concrete samples containing different amounts of pumice mineral which is a well-known light-weight structural material in Turkey (Yaltay et al., 2015), were presented. Total mass attenuation coefficient, mean free path and half value layer thickness values of concretes were determined via transmission experiments and simulations by using Geant4 code (Allison et al., 2016) at 511, 835 and 1275 keV photon energies. The web version of the well-known NIST XCOM code (Berger et al., 2010) was used for both comparison with experimental and simulation results, and for calculation of effective atomic numbers of concretes at 1 keV – 100 GeV photon energy range. The author thinks that this could be a good contribution to related literature from the aspect of using a Monte Carlo simulation code as a supporting tool to both experiments and theoretical calculations in such radiation research studies on mixtures such as concretes.

Since it is an attractive research field, one can find similar works on determination of radiation shielding properties of various materials via using similar procedures. However, some example studies can be listed as follows: Akkurt (2009) studied the effective atomic numbers of different types of steels by experiments and XCOM; Medhat et al. (2014) studied on Egyptian soils by using Geant4, FLUKA and XCOM; Taqi et al. (2017), also, studied on soils from Iraq experimentally, by XCOM and Geant4 codes; Vahabi et al. (2017) determined the mass attenuation coefficients of some polymers for several energies by XCOM and MCNP codes; Shamshad et al. (2017) made a study to investigate the gamma-ray shielding properties of Gadolinium based glasses on the basis of mass attenuation, effective atomic numbers and electron densities by using XCOM and Geant4; Bagheri et al. (2017) used XCOM and MCNP-4C codes for studying attenuation coefficients of Barium-Bismuth based glasses and in their study Ozyurt et al. (2018) calculated gamma-ray attenuation coefficients of some granite samples using GATE and XCOM for three energies.

2. Materials and Methods

2.1 Concretes

As abbreviation "PC" referring to "Pumice Concrete", three types of concretes were tested in the study, namely PC0, PC50 and PC100 which contains 0%, 50% and 100% pumice mineral, respectively. Pumice mineral was obtained from Isparta region. In the production of concretes Portland cement type 42.5 from Göltaş Plant established in Isparta was used. The water to cement ratio for all types of concretes was adjusted to ½. In Table 1, chemical compositions as weight fractions of constituent compounds and densities in grams per cm^3 of concretes were tabulated. Also, one can refer to Akkurt et al. (2010) to get related information about chemical properties of Portland cement.

Table 1. Chemical compositions of concrete samples.

Compound	PC0 (2.48 g/cm^3)	PC50 (1.83 g/cm^3)	PC100 (1.57 g/cm^3)
CaO	0.394	0.251	0.121
MgO	0.110	0.062	0.011
NaO	0.004	0.002	0.040
K_2O	0.000	0.000	0.008
Fe_2O_3	0.005	0.006	0.000
CO_2	0.315	0.164	0.560
SiO_2	0.127	0.095	0.094
H_2O	0.074	0.087	0.121
Al_2O_3	0.010	0.016	0.006
SO_2	0.005	0.005	0.000
$BaSO_4$	0.000	0.308	0.000
$CaCO_3$	0.000	0.007	0.000
MnO_2	0.000	0.001	0.000
NiO	0.000	0.001	0.000

2.2 μ/ρ by experiment

The total linear attenuation coefficients of pumice concretes were measured via a 3″×3″ NaI(Tl) detector connected to a 16k multichannel analyzer system manufactured by ORTEC. Figure 1 shows a schematic view of measurement setup. To fulfil the narrow-beam (or good geometry) conditions, two identical lead collimators, one after the source and one before the detector, were replaced in the measurements. Measurements were carried out for three photon energies from two well-known radioactive sources obtained from Spectrum Techniques Inc.: 835 keV from Manganese-54; 511 keV and 1275 keV from Sodium-22.

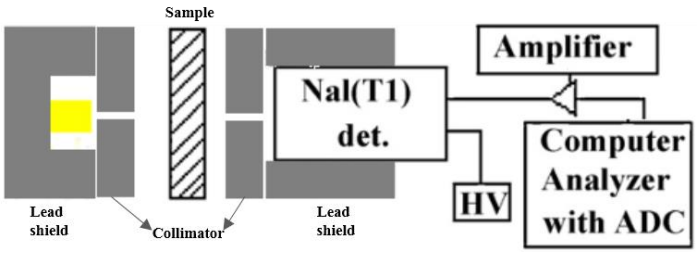

Figure 1. Schematic view of experimental setup (not to scale). The radioactive source is shown in yellow.

To determine the linear attenuation coefficient of a concrete sample Equation 2 was referred to. For this purpose, background subtracted intensities of photon beams with and without the concrete between the source and the NaI(Tl) detector were determined by using the ORTEC spectrum analysis software shipped with the system. For more detail on measurement system setup, one can refer to Akkurt et al. (2010). By using these experimental values of linear attenuation coefficients, mass attenuation coefficients were derived by dividing them to the densities of concretes. Then, *mfp,* and *HVL* values of concretes were calculated by using this mass attenuation data.

2.3 μ/ρ by XCOM calculation

To obtain theoretical values of total mass attenuation coefficients of concretes, the web version of XCOM photon cross section database was made use of. It is a database for calculation of photon cross sections of photoelectric effect, scattering (coherent and incoherent) and pair production (in nuclear and electron field), as well as the total attenuation coefficients (with and without coherent scattering) in mass attenuation form in the units of cm^2/g. The code currently works in 1 keV – 100 GeV photon energy range for compounds, mixtures and any pure element satisfying $Z \leq 100$ (Berger et al., 2010). For calculation of the total mass attenuation coefficients of concretes, chemical composition of each sample given in Table 1 was entered to XCOM as input. The energy range was selected as 1 keV – 100 GeV including 511, 835 and 1275 keV energies. In this step, tabulated total attenuation data without coherent scattering was taken into account. Depending on these values, variation of $Z_{eff,}$ *mfp* and *HVL* of concretes by photon energy were determined.

2.4 μ/ρ by Geant4 simulation

Simulation part of the study was realized by Geant4 (GEometry ANd Tracking, version 10.2) Monte Carlo simulation toolkit. It is an open source, object-oriented simulation code written in C++ language and can be freely provided from CERN (European Organization for Nuclear Research). Since it is capable of simulating the passage of many types of particles (for example photons, electrons, positrons, neutrons and ions) through matter in a wide energy span, it has a wide range of areas of application in nuclear, high energy, medical physics and radiation shielding design as well. At the heart of Geant4 are its physics models to handle particle-matter interactions across a wide range of energy, its geometry module to create even very complex geometries including material attributions and its particle tracking options including a list of useful detector types to collect requested information of any particle on propagation. Geant4 can simulate photon transportation from several eVs up to TeV region by means of several electromagnetic physics lists which include High Energy Physics models, Livermore evaluated data library and a C++ implementation of Penelope 2008 model (Allison et al., 2016; Geant4, 2018).

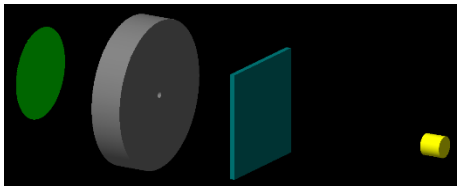

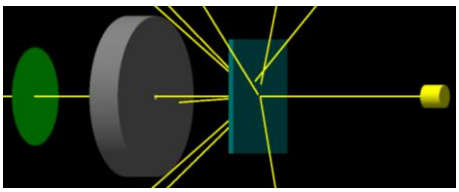

Figure 2. Sketch of simulation geometry (not to scale). From right to left: Source, sample, lead collimator and detecting region. Bottom figure, produced by OGL visualization driver, shows some transported photons at an instance.

Simulations were performed on a 64bit Fedora 27 platform. The geometry in the simulations, constructed by Geant4 *DetectorConstruction* class, was consisted of the source, sample, collimator and detector regions as can be seen in Figure 2. Geant4 material library was used for material assignments. The environment and collimator regions were filled with air and lead, respectively. The concrete materials were composed by entering the weight fractions given in Table 1 into Geant4 *DetectorConstruction* class. The source was created by using the *PrimaryGeneratorAction* class to randomly emit unidirectional photons of 511, 835 and 1275 keV energy towards the sample region. The purpose of the collimator was obtaining a parallel beam of uncollided photons to be counted only. In order to define a detector sensitive to photons, the *G4MultifunctionalDetector* class was implemented and a photon filter was attached to the detector which gave the result in *photons/mm*^{2}. In the study, standard electromagnetic physics list, implemented by the *G4EmPhysicsList* class, was used to manage photonic and electronic interactions. The fundamental photonic interactions, photoelectric effect, pair production in the field of nucleus and Compton scattering were taken into account by inclusion of *G4PhotoElectricEffect*, *G4GammaConversion*, *G4ComptonScattering* functions, respectively. Similarly, for simulation of necessary electronic processes *G4eBremsstrahlung*, *G4eIonisation*, *G4eMultipleScattering*, *G4eplusAnnihilation* functions were added for bremsstrahlung, ionization, multiple scattering and for annihilation of positrons, respectively. Besides these, fluorescence, Auger emission and particle induced X-ray emission effects were included. In simulations, the thresholds for secondary particle production processes (range cuts) was set to 0.1 mm for all particles in all materials. The total linear attenuation coefficients were calculated via Equation 2. For this purpose, sample region was first filled with air and then with related concrete material to estimate I_o and I, respectively. Using estimated μ values, mass attenuation coefficients, *mfp,* and *HVL* values for concretes were determined. Each simulation was carried out over 10^6 primary photons.

2.5 Z_{eff} calculation

In this part of the study, variation of effective atomic numbers of three types of concretes containing different amounts of pumice mineral was investigated by using the μ/ρ data obtained from XCOM code library at 1 keV – 100 GeV photon energy range. Z_{eff} values were calculated by a method named as the Direct Method which consists of the application of the following practical formula (Manohara et al., 2008).

$$Z_{eff} = \frac{\sum_i f_i A_i \left(\frac{\mu}{\rho}\right)_i}{\sum_i \frac{f_i A_i}{Z_i} \left(\frac{\mu}{\rho}\right)_i} \quad (6)$$

Here f_i, A_i, Z_i and $(\mu/\rho)_i$ correspond to the molar fraction, atomic weight, atomic number and mass attenuation coefficient of i^{th} constituent element in the concrete, respectively (İçelli and Erzenoğlu, 2004; Büyükyıldız, 2017).

3. Results and Discussion

In this study some essential radiation shielding parameters which are the total mass attenuation coefficients, effective atomic numbers, mean free paths and half value layer thicknesses, of concretes produced by pumice mineral were investigated using experimental (by a 16k NaI(Tl) detector system), Monte Carlo simulation (by Geant4 simulation toolkit) and calculation (by XCOM code) methods.

Shown in Figure 3 is the variation of the mass attenuation coefficients of investigated concretes in 1 keV – 100 GeV photon energy range. As seen from XCOM results, mass attenuation of each concrete follows a resembling pattern of variation. This pattern for each concrete is due to the reason that major photonic interactions dominates in different regions of energy because photoelectric effect, Compton scattering and pair production have different dependencies on incoming photon energy and atomic numbers of the constituent elements in that concrete (Jaeger, 1965; Chilton et al., 1984). Therefore, the width of the region that an interaction dominates changes by concrete type. At relatively low energies where photoelectric effect is predominant, sharp decreases at attenuation coefficients of the concretes are observed since occurrence of photoelectric effect is proportional to $Z^{4.5}$ and $1/E^3$ (Woods, 1982). Sudden increments seen are mainly due to the absorption of photons by *K* and *L* electronic shells for PC50 concrete; and by *K* shell for PC0 and PC100 concretes. In PC50 concrete, electronic shell contributions to photoelectric effect comes from the considerable relative amount of Barium element while in PC0 and PC100 concretes these contributions are due to the presence of Calcium content (Table 1). In this region PC50 concrete seems to be the most, PC100 concrete seems to be the least effective concrete.

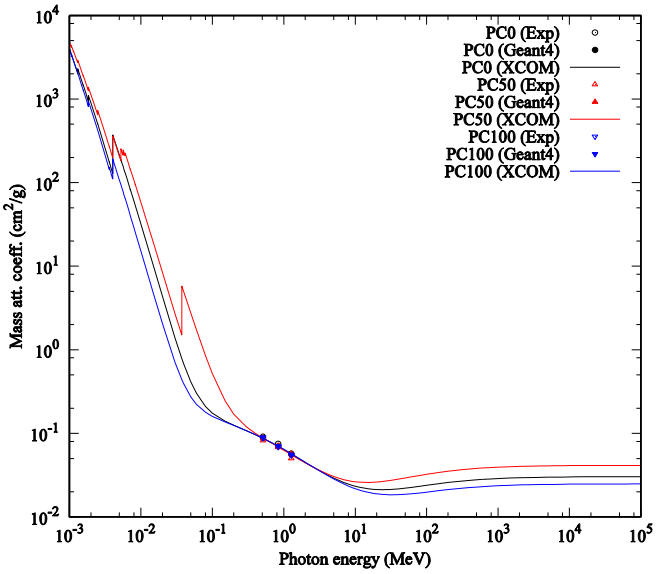

Figure 3. Variation of mass attenuation coefficients of pumice concretes by photon energy.

For moderate energies about 100 keV to 10 MeV, Compton scattering becomes predominant interaction mechanism where the mass attenuation coefficients vary slightly by energy. The reason is that the interaction cross section is proportional to *Z* and *1/E* (Woods, 1982). In this region, mass attenuation coefficients of all concretes lie very close to each other. Especially in between 0.5-6 MeV region, attenuation coefficients are so close that it can be argued that the cross sections per gram of each concrete are almost the equal. Attenuation coefficients obtained by experiments and simulations are also in this region. As can be seen from the figure, these values are in a good agreement with XCOM calculation values. The relative differences of experimental results with respect to XCOM were found to be ~10% for PC0, ~7% for PC50 and ~8% for PC100 concrete, while for simulations it was less than 2% for all concretes types, which indicates that simulation results are fairly close to calculation results. This situation about the magnitude of experimental errors when compared with the simulation case can be explained by reference to some unavoidable conditions of real-life transmission experiments such as probable heterogeneous structure of concrete samples, deflection of photon beam from narrow beam conditions and finally, counting statistics.

In the rest of the energy region starting from ~10 MeV where coefficients increase gradually, pair production is the dominant interaction. Interaction cross sections of concretes vary by Z^2 and at higher energies approximate to a constant value (Woods, 1982, Chilton et al., 1984). It can be said that PC50 concrete seems to be the most, PC100 concrete seems to be the least effective concrete in this region.

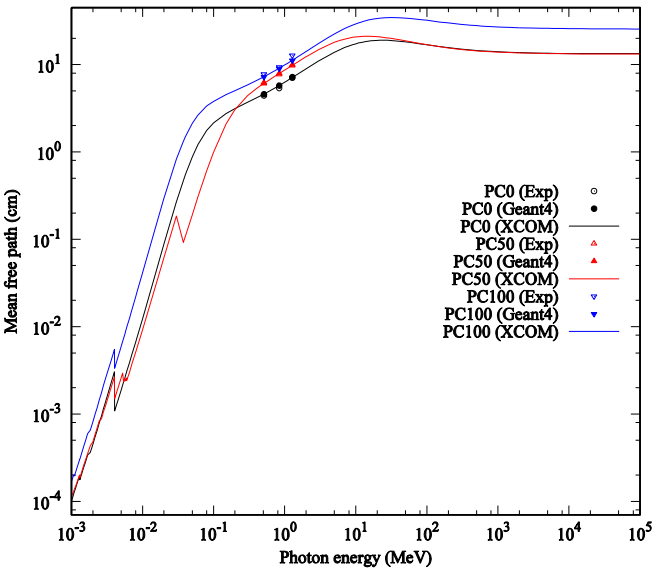

Figure 4. Variation of mean free path values of pumice concretes by photon energy.

In Figure 4 and 5, variations by photon energy of *mfp* and *HVL* values of concretes can be seen. Since both quantities are functions of $1/\mu$ (see Equation 4 and 5), they have similar trends of variation by energy. The values of *mfp* and *HVL* increase and decrease by decreasing and increasing values of linear attenuation coefficients. Sharp decreases are due to the *K, L* and *M* shells as discussed above. At very high energies, *mfp* and *HVL* values of PC0 and PC50 concretes converges, that is, for a particular energy the same thicknesses of these concretes approximately attenuates same fraction of incoming beam. At low energies PC50 is the most effective concrete type. Eventually, in the middle energy region PC0 concrete has the lowest *mfp* and *HVL* values because it has the highest density among all (Table 1).

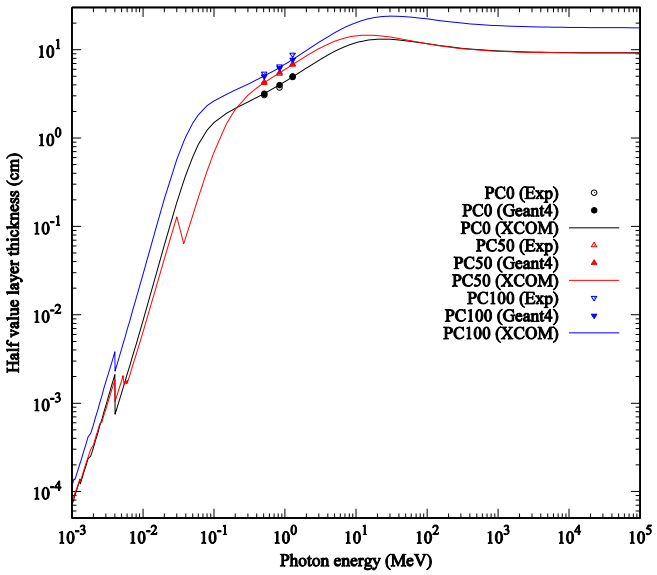

Figure 5. Variation of half value layer thicknesses of pumice concretes by photon energy.

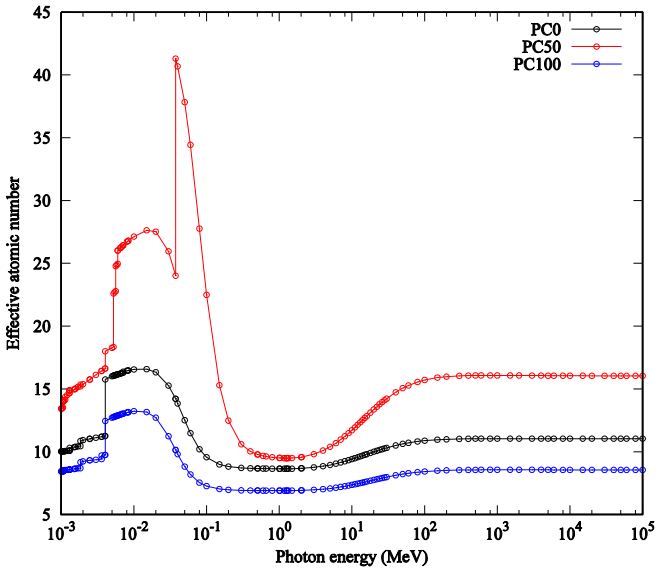

Figure 6. Variation of the effective atomic numbers of three types of pumice concretes by photon energy.

Variation by photon energy of the effective atomic numbers of three types of pumice concretes obtained from XCOM calculations are given in Figure 6. According to the figure, in all energy regions PC50 has the highest, PC100 has the lowest effective atomic number values. When overall variations are considered the patterns looks similar. For energies up to 4 - 5 keV, there is a slight increase in effective atomic number values for each concrete. The sudden increases for PC0 and PC100 concretes ~4 keV and for PC50 concrete around ~5 keV can be attributed to K electron shell contributions to mass attenuation coefficients from Calcium element. The remarkable peak belonging to PC50 concrete around ~35 keV can be attributed to contributions of K-shell electrons of Barium element which is not present in other two concrete types. For PC0 and PC100 concretes, approximately in 100 keV – 10 MeV energy region where Compton effect is the dominant interaction mechanism, Z_{eff} values remain almost constant. The same physical principle applies for PC50 concrete but it is clear that the energy region is narrower because of the greater Z_{eff} values PC50 has in this region. At the end of Compton effect dominant regions, Z_{eff} values of each concrete type show increases up to ~100 MeV photon energy, which can be ascribed to the mixed contribution of Compton effect with pair production to mass attenuation coefficients. After ~100 MeV, Z_{eff} values for all concretes approach to constant values where pair production effect becomes dominant.

4. Conclusions and Recommendations

Depending on the results and the discussions above, below conclusions and recommendations were listed.

- Depending on the mass attenuation coefficient, mean free path and half value layer thickness values, it can be concluded that PC50 concrete seems to be a better attenuator for low and very high photon energies where photoelectric and pair production effects are dominant, respectively. However, PC0 concrete would be advantageous in Compton effect dominant middle energy region since it has lower *mfp* and *HVL* values. PC100 concrete can be treated as the weakest attenuator among all concretes.
- Content of elements with high atomic masses contributes to attenuation capability of concretes in a positive way such as the presence of Barium in PC50 concrete. This effect can also be noticed at effective atomic number values. From this point of view, it can be stated that chemical property of a concrete has a strong effect on radiation shielding properties.
- The simulation results were found to be within a significantly low relative error. So, it can be concluded that Geant4 is a powerful tool to be used in such radiation shielding studies.
- Regarding the experimental errors, the author recommends that transmission experiments should be performed on different regions of the same concrete sample to minimize the probable error due to the impurity effects.

Acknowledgements

The author thanks TÜBİTAK (Türkiye Bilimsel ve Teknik Araştırma Kurumu) for its support to this study under project number 106M127.

References

Akkurt I. 2009. Effective atomic and electron numbers of some steels at different energies. Annals of Nuclear Energy 36, 1702-1705.

Akkurt I., Akyıldırım H., Mavi B., Kilincarslan S., Basyigit C. 2010. Photon attenuation coefficients of concrete includes barite in different rate. Annals of Nuclear Energy 37, 910-914.

Akman F., Durak R., Turhan M.F., Kaçal M.R. 2015. Studies on effective atomic numbers, electron densities from mass attenuation coefficients near the K edge in some samarium compounds. Applied Radiation and Isotopes 101, 107-113.

Allison J., Amako K., Apostolakis J., Arce P., Asai M., Aso T., Bagli E., Bagulya A., Banerjee S., Barrand G., Beck B.R., Bogdanov A.G., Brandt D., Brown J.M.C., Burkhardt H., Canal Ph., Cano-Ott D., Chauvie S., … Yoshida H. 2016 Recent developments in Geant4. Nuclear Instruments and Methods in Physics Research Section A: Accelerators, Spectrometers, Detectors and Associated Equipment. 835, 186-225.

Bagheri R., Moghaddam A.K., Yousefnia H. 2017. Gamma ray shielding study of barium-bismuth-borosilicate glasses as transparent shielding materials using MCNP-4C code, XCOM program, and available experimental data. Nuclear Engineering and Technology. 49, 216-223.

Berger M.J., Hubbell J.H., Seltzer S.M., Chang J., Coursey J.S., Sukumar R., Zucker D.S., and Olsen K. 2010. XCOM: photon cross section database (version 1.5). (Online) Available: http://physics.nist.gov/xcom. National Institute of Standards and Technology, Gaithersburg, MD. (accessed 20 March 2018).

Büyükyıldız M. 2017. Calculation of effective atomic numbers and electron densities of different types of material for total photon interaction in the continuous energy region via different methods. Sakarya University Journal of Science. 21(3), 314-323.

Chilton A.B., Shultis J.K., Faw R.E. 1984. Principles of radiation shielding, Prentice-Hall, Englewood Cliffs.

Elmahrough Y., Tellili B., Souga C. 2015. Determination of total mass attenuation coefficients, effective atomic numbers and electron densities for different shielding materials. Annals of Nuclear Energy 75, 268-274.

Geant4 A Simulation Toolkit. http://geant4.web.cern.ch/ (accessed 14 May 2018).

Hine G.J., 1952. The effective atomic numbers of materials for various gamma interactions. Physics Review 85, 725-737.

Hubbell, J.H. 1982. Photon mass attenuation and energy-absorption coefficients from 1 kev to 20 MeV. International Journal of Applied Radiations and. Isotopes. 33, 1269–1290.

İçelli O., Erzenoğlu S. 2004. Effective atomic numbers of some vanadium and nickel compounds for total photon interactions using transmission experiments. Journal of Quantitative Spectroscopy and Radiative Transfer. 85, 115-124.

Jaeger T. 1965. Principles of radiation protection engineering, McGraw-Hill Book Company, New York.

Kumar T.K., Reddy K.V. 1997. Effective atomic numbers for materials of dosimetric interest. Radiation Physics and Chemistry 50, 545-553.

Manohara S.R., Hanogodimath S.M., Thind K.S., Gerward L. 2008. On the effective atomic number and electron density: A comprehensive set of formulas for all types of materials and energies above 1 keV. Nuclear Instruments and Methods in Physics Research B. 266, 3906-3912.

Medhat M.E., Demir N., Tarim U.A., Gurler O. 2014. Calculation of gamma-ray mass attenuation coefficients of some Egyptian soil samples using Monte Carlo methods. Radiation Effects & Defects in Solids. 169(8), 706-714.

Murty V.R.K., Winkoun D.P., Devan K.R.S. 2000. Effective atomic numbers for W/Cu alloy using transmission experiments. Applied Radiation and Isotopes 53, 945-948.

Ozyurt O., Altinsoy N., Karaaslan Ş.İ., Bora A., Buyuk B., Erk İ. 2018. Calculation of gamma ray attenuation coefficients of some granite samples using a Monte Carlo simulation code. Radiation Physics and Chemistry. 144, 271-275.

Price B.T., Horton C.C., Spinney K.T. 1957. Radiation shielding, Pergamon Press Inc., London.

Shamshad L., Rooh G., Limkitjaroenporn P., Srisittipokakun N., Chaiphaksa W., Kim H.J., Kaewkhao J. 2017. A comparative study of gadolinium based oxide and oxyfluoride glasses as low energy radiation shielding materials. Progress in Nuclear Energy. 97, 53-59.

Taqi A.H. and Khalil H.J. 2017. An investigation on gamma attenuation of soil and oil-soil samples. Journal of Radiation Research and Applied Sciences. 10, 252-261.

Un A., Demir F. 2013. Determination of mass attenuation coefficients, effective atomic numbers and effective electron numbers for heavy-weight and normal-weight concretes. Applied Radiation and Isotopes 80, 73-77.

Woods J. 1982. Computational methods in reactor shielding, Pergamon Press Inc., New York.

Vahabi S.M., Bahreinipour M., Zafarghandi M.S. 2017. Determining the mass attenuation coefficients for some polymers using MCNP code: A comparison study. Vacuum. 136, 73-76.

Yaltay N., Ekinci C.E., Çakır T., Oto B. 2015. Photon attenuation properties of concrete produced with pumice aggregate and colemanite addition in different rates and the effect of curing age to these properties. Progress in Nuclear Energy 78, 25-35.